Low-Cost Bioadsorbents for the Removal of Aqueous Effluents

Amir Djellouli
Laboratory of Physics, Matter and Radiation, Department of Process Engineering, Faculty of Science and Technology, University Mohammed Cherif Messaadia, Souk-Ahras, Algeria
a.djellouli@univ-soukahras.dz (corresponding author)

Yamina Berredjem
Laboratory of Water Treatment and Valorization of Industrial Wastes, Department of Chemistry, Faculty of Science, University Badji Mokhtar, Annaba, Algeria
y.berredjem@univ-soukahras.dz

Mohamed Yagoub
Hydraulic Development and Environment Laboratory, University of Biskra, Biskra 07000, Algeria
m.yagoub@univ-biskra.dz

Received: 16 March 2025 | Revised: 8 April 2025 | Accepted: 22 April 2025

 DOI: https://doi.org/10.48084/etasr.10970

ABSTRACT

This study aimed to synthesize and manufacture Sunflower Seed Hull Biochar (SSHB690) as a promising, cost-effective, and eco-friendly adsorbent for removing 4-Nitrophenol (4-NP) from aqueous solutions. Several characterization techniques were used to analyze this biosorbent, including X-Ray Diffraction (XRD), Scanning Electron Microscopy (SEM), Brunauer-Emmett-Teller (BET), and Fourier Transform Infrared (FTIR) spectroscopy. The batch testing considered factors, such as temperature, pH, concentration, contact time, and material dose. The best removal of 4-NP was achieved at 25 °C (298 K) and pH = 5.5, yielding a maximum removal efficiency of 95%. The adsorption data fitted best with the Liu isotherm model with the highest Q_{max} and R^2 value, while the kinetic studies showed that the adsorption rate followed Pseudo-Second-Order (PSO). The thermodynamic parameters confirmed that the adsorption process was exothermic ($\Delta H^\circ < 0$) and spontaneous ($\Delta G^\circ < 0$).

Keywords-SSHB690; wastewater; 4-nitrophenol; kinetics; adsorption

I. INTRODUCTION

The rapid growth of industrial activities worldwide has led to the spread of different organic and inorganic contaminants in aquatic environments posing a serious environmental issue. For instance, the effluents of the textile industry include mostly synthetic dyes, which are typically overused in the dying process to enhance the intensity of color. As a result, wastewater from this kind of industries contains high concentrations of persistent compounds. Due to their complex aromatic components, these dyes are resistant to biodegradation and persist in the environment for a high period time. Similarly, heavy metals in these contaminated waters are extremely toxic even at very low concentrations, threatening aquatic and human life [1, 2]. Contaminated water must, therefore, be cleaned before being disposed into the sewage system.

To address this issue, several methods have been developed to effectively remove the aforementioned effluents from aqueous media, including advanced oxidation, microbiological biodegradation, photodegradation, ozonation, and photocatalysis. However, these techniques are often expensive and energy-intensive, especially for high quantities of contaminated water. In contrast, the adsorption process, when using inexpensive adsorbents like industrial and agricultural waste, has emerged as a promising method for removing pollutants from aqueous media.

Nitrophenols and other Nitroaromatic Compounds (NACs) are widely employed in the synthesis of pesticides, dyes, and pharmaceuticals and are also formed as byproducts during their degradation [3]. These compounds are extremely dangerous due to their ecotoxicity, mutagenicity, carcinogenicity, and reproductive toxicity. They are metabolized by microbes in the liver or intestines, resulting in toxic and carcinogenic metabolites [4]. To lessen these threats, the effective removal of NACs from the environment becomes necessary [5, 6].

Although being a practical solution, biological treatment techniques do not fully degrade these pollutants [7]. Chemical coagulation and catalytic reduction, especially to transform 4-NP into less toxic compounds, such as 4-Aminophenol (4-AP), have been considered as alternatives [8-11]. However, these

methods can also be expensive and might not be suitable for common use. Adsorption remains the most suitable method due to its affordability, ease of use, and environmental friendliness [12-20].

Biochar is a carbonaceous solid produced by pyrolysis of biomass and has shown great potential for phenolic compound adsorption in wastewater treatment. Although it has a smaller surface area than activated carbon when produced at 500-600 °C, it has more surface functionality, which improves its adsorption capabilities [21, 22].

II. MATERIALS AND METHODS

A. Adsorbent

Sunflower Seed Hulls (SSH) were utilized as waste materials collected from an oasis in Biskra, Algeria. The hulls were washed with distilled water several times to remove any dirt or impurities and were dried under the sun. After this, they were chopped into few pieces and further dried in an oven for 48 hours at 110 °C. The dried material was grounded until particles were sized between 0.08 and 0.2 mm.

The prepared materials were pyrolyzed in a crucible coated with porcelain under an oxygen-restricted atmosphere. The heating process entailed gradual temperature increase from room temperature to 690 °C at a rate of 10 °C per min, maintained for three hours.

Following pyrolysis, biochar was sumberged in a 0.1 M HCl solution and washed well with hot, deionized water until the pH of the filtrate was neutral. The treated biochar, reffered to as SSHB690, was dried for 24 hours at 110 °C to keep its moisture content below 5%. The final product was stored in a desiccator until it was further used.

B. Adsorbates

All of the chemicals and reagents utilized in this investigation were of 99% reagent grade and were acquired from Sigma-Aldrich. The primary adsorbate selected was 4-NP, a phenolic compound with the chemical formula $C_6H_5NO_3$ and a molecular weight of 139.11 g/mol. Its CAS number is 100-02-7 (Sigma-Aldrich, lot #MKBV0501V). All solutions and compounds were prepared using deionized water and were utilized without additional purification.

C. Sample Characterization

FTIR spectroscopy was deployed to examine the surface characteristics of the synthetic biochar. Spectra were obtained between 400 and 4000 cm^{-1} using the Shimadzu IRAffinity-1 with the KBr pellet method.

The structure was assessed through XRD analysis using a PANalytical diffractometer with Cu Kα radiation (λ = 1.5406 Å) at 30 mA and 40 kV. SEM and Energy Dispersive X-ray Spectroscopy (EDS) using a TESCAN VEGA3 system, were utilized to identify the components of the generated sample and ascertain its surface structure in a scanning range of 2°-70°.

The total pore volume (V_{total}) and specific surface area (S_{BET}) were determined using the N_2 adsorption-desoprtion isotherm at 77 K, measured with the ASAP 2020 analyzer. BET was applied for surface area calculation, while Barrett-Joyner-Halenda (BJH) was used to evaluate the micropore characteristics from the desorption isotherm.

The pH of Point of Zero Charge (pHPZC) was determined based on the method described in a previous study [23]. The initial pH (pH_0) of 50 mL of 0.01 M NaCl solution was adjusted to a range of 2-12 using HCl or NaOH. After adding 50 mg of SSHB690 to each solution, the mixture was stirred overnight at room temperature. The final pH (pH_f) was recorded and the direct determination of the pHPZC values was achieved by plotting the difference pH_f - pH_0 against pH_0.

D. Adsorption Experiments

Adsorption experiments were conducted in a batch system at 298 K, except for temperature variation studies. A stock solution of 0.5 g/L was used to prepare all solutions. In each experiment, 30 mL of 4-NP and 30 mg of SSHB690 adsorbent were added to 50 mL Erlenmeyer flasks. The mixtures were agitated at a constant speed of 300 rpm for a predetermined contact time. The loaded adsorbent was filtered out using a 0.25 µm membrane and the residual mount concentration of 4-NP in the solution was then measured using UV-Vis spectrophotometry at 415 nm.

III. RESULTS AND DISCUSSION

A. Brunauer-Emmett-Teller *and Barrett-Joyner-Halenda Analysis*

Table I presents the results of BET and BJH analysis for both SSH and SSHB690 wastes.

TABLE I. BET AND BJH RESULTS OF SSH AND SSHB690

Adsorbant	S_{BET} (m^2/g)	V_{total} (cm^3/g)
SSH	3.7315	0.000017
SSHB690	388.0277	0.224263

The SSH exhibited a very low surface area and negligible porosity. After pyrolysis, the biochar SSHB690 had significant higher surface area and total pore volume, confirming the potential of SSHB690 for adsorption applications.

B. Scanning Electron Microscopy Micrographs

The surface of raw SSH appeared mostly smooth, with few visible pores. On the other hand, the SSHB690 surface exhibited a much greater number of pores with different widths and noticeable dispersion. This can be related to the degradation of cellulose and lignin inside the biochar structure, changing the structure [24].

C. Fourier Transform Infrared Analysis

FTIR spectroscopy was employed to identify the surface functional groups of the adsorbents. Regarding SSHB690, compounds with triple bonds (C≡C) and nitriles (C≡N) can serve as indicators of functional groups that are either created or maintained throughout the activation process. The carbon can effectively capture certain pollutants, particularly organic contaminants and gases, as these groups increase the carbon's polarity and adsorption capacity. Furthermore, the presence of CO_2 in the 230-2400 cm^{-1} range is frequently caused by atmospheric interference rather than a material's inherent characteristics.

In SSH, the spectrum displayed O-H stretching vibrations, C-H deformations, C=O stretching, and C-O stretching vibrations. The results were similar to those of [25], indicating that pyrolysis not only changed the physical structure, but also chemically activated the adsorbent, improving its effectiveness in capturing heavy metals and other contaminants.

D. X-Ray Diffraction Analysis

A prominent peak in 2θ at roughly 20°-25° was detected in the spectrum for SSH (raw biomass). This peak indicated the presence of semi-crystalline or amorphous organic materials, such as cellulose, hemicellulose, and lignin, which have some degree of short-range structure. In SSHB690, the spectrum's peaks were softer and less discernible. The HCl activation of the biomass disrupted its ordered structure, transforming the organic molecules into a highly porous and disorganized material. This resulted in a higher specific surface area as well as multiple adsorption active sites. The material's porosity caused the peaks to broaden and the diffraction intensity to decrease, suggesting a more porous and disordered structure.

In conclusion, raw biomass's XRD spectrum exhibited some degree of organization and crystallinity, whereas activated carbon's spectrum, which is the consequence of the biomass's chemical activation and thermal degradation, displayed a highly porous and disordered structure [26].

IV. EFFECT OF OPERATIONAL PARAMETERS ON 4-NP ADSORPTION

A. Effet of Time

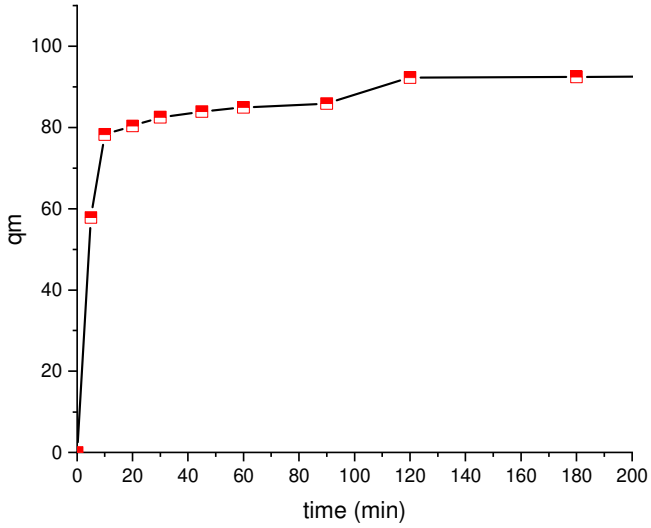

Fig. 1. Effect of contact time.

To determine the cost of the adsorption process, the contact time of this procedure was determined. Figure 1 illustrates the variation in 4-NP adsorption on SSHB690 biochar over a range of contact times (5-200 min). The findings demonstrated a two-stage dye adsorption. During the initial phase (0-60 min), a rapid increase in adsorption was observed. This can be attributed to the adsorption of pollutant molecules in a large number of free active sites. Other ions could not enter the solution as the pores closed. After this period, the adsorption slowed down and after 120 min, equilibrium was reached. SSHB690 removed about 86.42% of the total pollutant content [27-29].

B. Effet of pH

The competitive interaction between excess protons (H^+) and 4-NP ions to occupy active sites on the SSHB690 surface may be the cause of the lower adsorption efficiency of 4-NP in acidic environments. Figure 2 indicated that the adsorption efficiency of 4-NP increased significantly from 93.84% to 20.98% as the pH of the initial solution increased, having reached a maximum at pH = 3.62 before having declined to 11. The decrease in the concentration of H^+ ions in the solution, which reduced this competition by raising the negative charge of the surface, is what caused the observed increase in the percentage removal of 4-NP with increasing pH values up to 5.6.

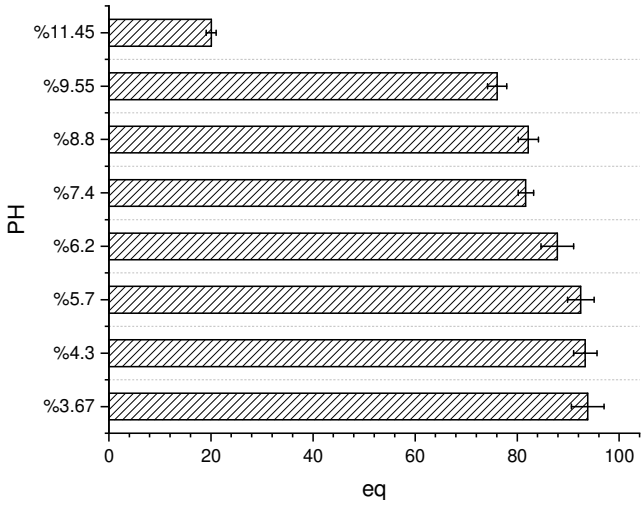

Fig. 2. Effet of PH.

At pH > 6, 4-NP ions began to dissipate as precipitation took place. The pHPZC revealed that the surface of the biochar was negatively charged when the pH was greater than pHPZC, which encouraged the uptake of CV dye in the solution. However, the surfaces of the two adsorbents became positive when the pH fell below pHPZC, which makes it difficult for cationic dyes, like CV dye, to adsorb [30].

C. Modeling of Isotherms

A comparison of the calculated isotherm coefficients, as displayed in Figure 3 and Table II, demonstrated that equilibrium adsorption data fit best with the Liu isotherm model, as indicated by the lowest reduced chi-square ($red\text{-}\chi^2$ = 41.376) and highest adjusted R^2 ($adj\text{-}R^2$ = 0.9876),compared to the Langmuir and Temkin models. This suggests that the adsorption of 4-NP on SSHB690 occurred on a homogeneous surface and was driven by a monolayer process. The maximum adsorption capacity of the Langmuir model, Q_{max} = 244.48 mg/g, and the determined separation factor, K_L = 0.0748 L/mg, both indicated a satisfactory adsorption process. Furthermore, the data were well-fitted by the Freundlich model ($adj\text{-}R^2$ = 0.988).

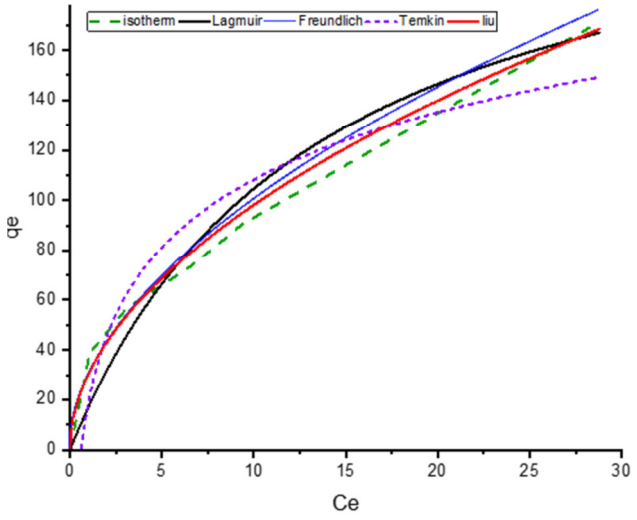

Fig. 3. Modeling of Isotherms.

TABLE II. ISOTHERM PARAMETERS FOR THE ADSORPTION OF 4-NP ON SSHB690

Model	Parameters	Unit	Value
Langmuir	Q_{max}	mg/g	244.48 ± 42.85
	K_L	L/mg	0.0748 ± 0.027
	adj-R^2	-	0.9461
	red-χ^2	-	179.74
Freundlich	K_F	(mg/g)·(mg/L$^{1/n}$)	29.30 ± 0.24
	n_F	-	1.875 ± 0.0101
	adj-R^2	-	0.988
	red-χ^2	-	28.327
Temkin	A_T	L/mg	1.6212 ±0.783
	B_T	J/mol	38.848 ± 7.56
	adj-R^2	-	0.896
	red-χ^2	-	345.473
Liu	q_m	mg/g	134,669.89 ± 6.26
	k	-	7.34E-8 ± 6.73E-5
	n	-	0.5113± 0.195
	adj-R^2	-	0.9876
	red-χ^2	-	41.376

Compared to the Freundlich and Langmuir models, the Temkin isotherm exhibited a lower correlation coefficient. The Temkin isotherm, linked to the heat of adsorption, indicated evidence of chemisorption due to its value exceeding 8 kJ L^{-1} [31].

D. Kinetic Model Fitting

TABLE III. THERMODYNAMIC PARAMETERS FOR 4-NP ADSORPTION ON SSHB690.

T (K)	Q_{max} (mg/g)	ΔS (J/mol)	ΔG (kJ/mol)	ΔH (kJ/mol)
393	76.93	-22.81	-3.127	-10.012
303	88.56		-2.867	
313	69.27		-2.456	

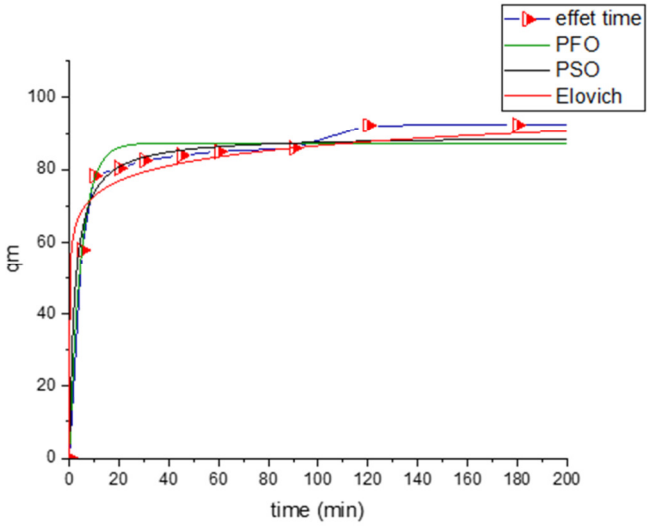

Fig. 4. Kinetic model fitting.

TABLE IV. KINETIC PARAMETERS FOR THE ADSORPTION OF 4-NP ON SSHB690

Model	Parameters	Unit	Value
Pseudo-First Order (PFO)	q_e	mg/g	87.19 ± 1.49
	k_1	min^{-1}	0.216 ± 0.02
	adj-R^2	-	0.976
	red-χ^2	-	172.944
Pseudo-Second Order (PSO)	q_e	mg/g	89.36 ± 0.09
	k_2	g/(min mg)	0.005 ± 9.86
	adj-R^2	-	0.927
	red-χ^2	-	5.433
Elovich	α	g/(min mg)	105,656 ± 25,380.64
	β	mg/g	0.16608 ± 0.003
	adj-R^2	-	0.778
	red-χ^2	-	14.423

V. CONCLUSION

The goal of this study was to develop a novel adsorbent material, Sunflower Seed Hull Biochar (SSHB690), derived from agricultural waste, specifically Sunflower Seed Hulls (SSH) from the Biskra region, to effectively remove 4-Nitrophenol (4-NP) from aqueous solutions. After approximately 120 min at a pH of 5.5, the adsorption efficiency of 4-NP solution reached an impressive 95%. This result highlighted the potential of using agricultural byproducts for environmental cleanup applications.

The surface analysis of SSHB690 revealed a significant increase in surface area (S_{BET} = 388.03 m²/g) compared to the raw SSH (S_{BET} = 3.73 m²/g). The X-Ray Diffraction (XRD) analysis confirmed that the material's structure was amorphous carbon, while Fourier Transform Infrared (FTIR) spectroscopy detected several oxygen-bonded functional groups on the surface. These features were indicative of the material's high adsorption capacity.

The adsorption process was modeled using Liu's adsorption isotherm, which exhibited that the maximum adsorption capacity for SSHB690 was Q_{max} = 134,669.89 mg/g. This

suggested that a monolayer adsorption mechanism was involved, supporting a homogeneous process. Kinetic studies further revealed that although the Pseudo-First-Order (PFO) model exhibited better correlation (highest R^2 value), the Pseudo-Second-Order (PSO) model gave a more accurate prediction (lower *red-*χ^2), which suggests that it may better represent the actual adsorption mechanism. The thermodynamic parameters confirmed that the adsorption process was exothermic ($\Delta H° < 0$) and spontaneous ($\Delta G° < 0$).

This study demonstrates the potential of transforming SSH waste into valuable activated carbon, promoting sustainability and circular economy practices. It also presents an opportunity for job creation in regions where sunflower seeds are produced. Future research should focus on optimizing production conditions for activated carbon, and field trials should be conducted to assess its performance in real-world applications, such as industrial wastewater treatment facilities.

REFERENCES

[1] S. H. Abro, H. A. Moria, A. Chandio, and A. Z. Al-Khazaal, "Understanding the Effect of Aluminum Addition on the Forming of Second Phase Particles on Grain Growth of Micro-Alloyed Steel," *Engineering, Technology & Applied Science Research*, vol. 10, no. 1, pp. 5153–5156, Feb. 2020, https://doi.org/10.48084/etasr.3243.

[2] K. Khaskhoussy, B. Kahlaoui, B. M. Nefzi, O. Jozdan, A. Dakheel, and M. Hachicha, "Effect of Treated Wastewater Irrigation on Heavy Metals Distribution in a Tunisian Soil," *Engineering, Technology & Applied Science Research*, vol. 5, no. 3, pp. 805–810, Jun. 2015, https://doi.org/10.48084/etasr.563.

[3] Y. Du, M. Zhou, and L. Lei, "Role of the intermediates in the degradation of phenolic compounds by Fenton-like process," *Journal of Hazardous Materials*, vol. 136, no. 3, pp. 859–865, Aug. 2006, https://doi.org/10.1016/j.jhazmat.2006.01.022.

[4] N. Wan, J.-D. Gu, and Y. Yan, "Degradation of *p*-nitrophenol by *Achromobacter xylosoxidans* Ns isolated from wetland sediment," *International Biodeterioration & Biodegradation*, vol. 59, no. 2, pp. 90–96, Mar. 2007, https://doi.org/10.1016/j.ibiod.2006.07.012.

[5] Z. Pei, X. Shan, B. Wen, S. Zhang, L. Yan, and S. U. Khan, "Effect of copper on the adsorption of *p*-nitrophenol onto soils," *Environmental Pollution*, vol. 139, no. 3, pp. 541–549, Feb. 2006, https://doi.org/10.1016/j.envpol.2005.05.025.

[6] D. Sreekanth, D. Sivaramakrishna, V. Himabindu, and Y. Anjaneyulu, "Thermophilic degradation of phenolic compounds in lab scale hybrid up flow anaerobic sludge blanket reactors," *Journal of Hazardous Materials*, vol. 164, no. 2, pp. 1532–1539, May 2009, https://doi.org/10.1016/j.jhazmat.2008.09.070.

[7] Ö. Aktaş and F. Çeçen, "Adsorption and cometabolic bioregeneration in activated carbon treatment of 2-nitrophenol," *Journal of Hazardous Materials*, vol. 177, no. 1, pp. 956–961, May 2010, https://doi.org/10.1016/j.jhazmat.2010.01.011.

[8] S. H. Lin and C. S. Wang, "Treatment of high-strength phenolic wastewater by a new two-step method," *Journal of Hazardous Materials*, vol. 90, no. 2, pp. 205–216, Mar. 2002, https://doi.org/10.1016/S0304-3894(01)00351-X.

[9] A. O. Cardoso Juarez, E. Ivan Ocampo Lopez, M. K. Kesarla, and N. K. R. Bogireddy, "Advances in 4-Nitrophenol Detection and Reduction Methods and Mechanisms: An Updated Review," *ACS Omega*, vol. 9, no. 31, pp. 33335–33350, Aug. 2024, https://doi.org/10.1021/acsomega.4c04185.

[10] Y. Rodriguez Mejía and N. K. R. Bogireddy, "Reduction of 4-nitrophenol using green-fabricated metal nanoparticles," *RSC Advances*, vol. 12, no. 29, pp. 18661–18675, 2022, https://doi.org/10.1039/D2RA02663E.

[11] R. D. Neal, Y. Inoue, R. A. Hughes, and S. Neretina, "Catalytic Reduction of 4-Nitrophenol by Gold Catalysts: The Influence of Borohydride Concentration on the Induction Time," *The Journal of Physical Chemistry C*, vol. 123, no. 20, pp. 12894–12901, May 2019, https://doi.org/10.1021/acs.jpcc.9b02396.

[12] Y. Qu, L. Yu, B. Zhu, F. Chai, and Z. Su, "Green synthesis of carbon dots by celery leaves for use as fluorescent paper sensors for the detection of nitrophenols," *New Journal of Chemistry*, vol. 44, no. 4, pp. 1500–1507, Jan. 2020, https://doi.org/10.1039/C9NJ05285B.

[13] S. J. Lee, Y. Yu, H. J. Jung, S. S. Naik, S. Yeon, and M. Y. Choi, "Efficient recovery of palladium nanoparticles from industrial wastewater and their catalytic activity toward reduction of 4-nitrophenol," *Chemosphere*, vol. 262, Jan. 2021, Art. no. 128358, https://doi.org/10.1016/j.chemosphere.2020.128358.

[14] A. Saravanan *et al.*, "A comprehensive review on sources, analysis and toxicity of environmental pollutants and its removal methods from water environment," *Science of The Total Environment*, vol. 812, Mar. 2022, Art. no. 152456, https://doi.org/10.1016/j.scitotenv.2021.152456.

[15] J. O. Ighalo *et al.*, "Recent advances in hydrochar application for the adsorptive removal of wastewater pollutants," *Chemical Engineering Research and Design*, vol. 184, pp. 419–456, Aug. 2022, https://doi.org/10.1016/j.cherd.2022.06.028.

[16] H. T. Hamad, "Removal of phenol and inorganic metals from wastewater using activated ceramic," *Journal of King Saud University - Engineering Sciences*, vol. 33, no. 4, pp. 221–226, May 2021, https://doi.org/10.1016/j.jksues.2020.04.006.

[17] M. A. Al-Ghouti *et al.*, "Effective removal of phenol from wastewater using a hybrid process of graphene oxide adsorption and UV-irradiation," *Environmental Technology & Innovation*, vol. 27, Aug. 2022, Art. no. 102525, https://doi.org/10.1016/j.eti.2022.102525.

[18] S. Bousba and A. H. Meniai, "Removal of Phenol from Water by Adsorption onto Sewage Sludge Based Adsorbent," *Chemical Engineering Transactions*, vol. 40, pp. 235–240, Sep. 2014, https://doi.org/10.3303/CET1440040.

[19] E. E. P. Ramírez *et al.*, "Removal of Phenolic Compounds from Water by Adsorption and Photocatalysis," in *Phenolic Compounds - Natural Sources, Importance and Applications*, London, UK: IntechOpen, 2017.

[20] S. J. Kulkarni and J. P. Kaware, "Review on research for removal of phenol from wastewater," *International journal of scientific and research publications*, vol. 3, no. 4, pp. 1–5, Apr. 2013.

[21] Y. S. Dzyazko *et al.*, "Nanoporous Biochar for Removal of Toxic Organic Compounds from Water," in *Nanophotonics, Nanooptics, Nanobiotechnology, and Their Applications*, Cham, Switzerland, 2019, pp. 209–224, https://doi.org/10.1007/978-3-030-17755-3_14.

[22] K. Sun, K. Ro, M. Guo, J. Novak, H. Mashayekhi, and B. Xing, "Sorption of bisphenol A, 17α-ethinyl estradiol and phenanthrene on thermally and hydrothermally produced biochars," *Bioresource Technology*, vol. 102, no. 10, pp. 5757–5763, May 2011, https://doi.org/10.1016/j.biortech.2011.03.038.

[23] A. Naima *et al.*, "Development of a novel and efficient biochar produced from pepper stem for effective ibuprofen removal," *Bioresource Technology*, vol. 347, Mar. 2022, Art. no. 126685, https://doi.org/10.1016/j.biortech.2022.126685.

[24] N. Rouahna *et al.*, "Reduction of Crystal Violet Dye from Water by Pomegranate Peel–Derived Efficient Biochar: Influencing Factors and Adsorption Behaviour," *Water, Air, & Soil Pollution*, vol. 234, no. 5, May 2023, Art. no. 324, https://doi.org/10.1007/s11270-023-06338-0.

[25] N. Maaloul, P. Oulego, M. Rendueles, A. Ghorbal, and M. Díaz, "Synthesis and characterization of eco-friendly cellulose beads for copper (II) removal from aqueous solutions," *Environmental Science and Pollution Research*, vol. 27, no. 19, pp. 23447–23463, Jul. 2020, https://doi.org/10.1007/s11356-018-3812-2.

[26] N. U. M. Nizam, M. M. Hanafiah, E. Mahmoudi, A. A. Halim, and A. W. Mohammad, "The removal of anionic and cationic dyes from an aqueous solution using biomass-based activated carbon," *Scientific Reports*, vol. 11, no. 1, Apr. 2021, Art. no. 8623, https://doi.org/10.1038/s41598-021-88084-z.

[27] C. Bai, L. Wang, and Z. Zhu, "Adsorption of Cr(III) and Pb(II) by graphene oxide/alginate hydrogel membrane: Characterization, adsorption kinetics, isotherm and thermodynamics studies,"

International Journal of Biological Macromolecules, vol. 147, pp. 898–910, Mar. 2020, https://doi.org/10.1016/j.ijbiomac.2019.09.249.

[28] S. Bhowmik, V. Chakraborty, and P. Das, "Batch adsorption of indigo carmine on activated carbon prepared from sawdust: A comparative study and optimization of operating conditions using Response Surface Methodology," *Results in Surfaces and Interfaces*, vol. 3, May 2021, Art. no. 100011, https://doi.org/10.1016/j.rsurfi.2021.100011.

[29] Y. L. Salomón *et al.*, "Adsorption of atrazine herbicide from water by diospyros kaki fruit waste activated carbon," *Journal of Molecular Liquids*, vol. 347, Feb. 2022, Art. no. 117990, https://doi.org/10.1016/j.molliq.2021.117990.

[30] M. Abbas, Z. Harrache, and M. Trari, "Removal of gentian violet in aqueous solution by activated carbon equilibrium, kinetics, and thermodynamic study," *Adsorption Science & Technology*, vol. 37, no. 7–8, pp. 566–589, Oct. 2019, https://doi.org/10.1177/0263617419864504.

[31] A. Khamwichit, W. Dechapanya, and W. Dechapanya, "Adsorption kinetics and isotherms of binary metal ion aqueous solution using untreated venus shell," *Heliyon*, vol. 8, no. 6, Jun. 2022, Art. no. e09610, https://doi.org/10.1016/j.heliyon.2022.e09610.